# Supplemental Material for:
# Bosonic Analogue of Dirac Composite Fermi Liquid

## COUPLED-WIRE CONSTRUCTION OF BOSONIC INTEGER QUANTUM HALL STATE

In the main text, we used strips of bosons at $\nu = 2$ as a building block for our network model of a quantum Hall plateau transition. It is useful to view each such strip in Fig. 2(a) of the main text as itself composed of quantum wires [1] labeled by $j = 1, \ldots, N$. Each wire hosts charge-$e$ bosons $\sim e^{i\varphi_j}$ described by

$$\mathcal{L}_{\text{wire}} = \frac{\partial_x \theta_j}{\pi}(\partial_t \varphi_j - A_0) + \frac{v}{2\pi}[(\partial_x \varphi_j - A_1)^2 + (\partial_x \theta_j)^2]$$

where $\frac{\partial_x \theta_j}{\pi}$ is conjugate to $\varphi_j$. When a boson hops between neighboring wires at non-zero magnetic field—conveniently taken in the gauge $A_2 = Bx$—it acquires an Aharonov-Bohm phase $\exp[i\frac{2\pi edB}{hc}x]$ that prevents condensate formation. These oscillating phases can be compensated, however, when a phase slip $\sim e^{2i\theta + i2\pi d\rho_0 x}$ accompanies boson hopping. For $\nu = 2$ this occurs for second-neighbor hopping described by

$$\mathcal{L}_{\text{boson IQH}} = g_{\text{IQH}} \sum_j \cos\left(\varphi_{j+1} - \varphi_{j-1} + 2\theta_j\right). \quad (1)$$

A bosonic IQH state with $\sigma_{xy} = 2e^2/h$ [2–4] emerges when $g_{\text{IQH}}$ flows to strong coupling. The $\nu = 2$ strip then hosts edge states with two flavors $\alpha = \pm$ of charge-$e$ bosons $b_{y=1(2),\alpha} \sim e^{i\phi_{y=1(2),\alpha}}$ at the lower (upper) edge, where

$$\begin{aligned} \phi_{y=1,+} &\equiv \varphi_1, & \phi_{y=1,-} &\equiv \varphi_2 + 2\theta_1, \\ \phi_{y=2,+} &\equiv \varphi_{N-1} - 2\theta_N, & \phi_{y=2,-} &\equiv \varphi_N. \end{aligned} \quad (2)$$

The Lagrangian density for the lower and upper edges is succinctly written as

$$\mathcal{L}_{\text{edge}} = \frac{(-1)^y K_{\alpha\alpha'}}{4\pi} \partial_x \phi_{y,\alpha} \partial_t \phi_{y,\alpha'} + \frac{u}{4\pi}\left(\partial_x \phi_{y,\alpha}\right)^2, \quad (3)$$

where $K = \sigma^x$, and $\alpha, \alpha'$ are implicitly summed over. This is the edge theory for the boson IQH strips used in the main text and generalizes straightforwardly to the full 2D system in Fig. 2(a) when edges are enumerated by integers $y$. The more microscopic picture provided here allows us in particular to consider microscopic inversion symmetry and verify its action on the low-energy edge fields quoted in the main text.

## GENERAL COMPOSITE-FERMION BAND STRUCTURE

In the absence of any symmetry, the most general momentum-independent bilinear perturbations to the composite-fermion Hamiltonian

$$H_0 = \Psi_4^\dagger(\sigma^x k_1 + \sigma^y k_2)\Psi_4 \quad (4)$$

are given by

$$\delta H = \sum_{\alpha,\beta=0,x,y,z} c_{\alpha\beta} \hat{h}_{\alpha\beta}, \quad (5)$$

$$\hat{h}_{\alpha\beta} \equiv \Psi_4^\dagger \sigma^\alpha \tau^\beta \Psi_4, \quad (6)$$

where $c_{\alpha\beta}$ are real constants. We now discuss these terms according to their symmetries:

1. **Particle-hole symmetry broken.** The six terms $\hat{h}_{i0}$ and $\hat{h}_{0i}$ with $i = x, y, z$, are odd under particle-hole symmetry. Among these, $\hat{h}_{x/y,0}$ and $\hat{h}_{0,x/y}$ break rotation symmetry; the former moves the Dirac cones in momentum while the latter splits them in energy. The terms $\hat{h}_{z0}$ and $\hat{h}_{0z}$ are rotation symmetric; the former opens a gap while the latter is a chemical potential with opposite sign for the two cones.

2. **Particle-hole and rotation symmetries.** The combination of particle-hole and (fourfold) rotation symmetry allows only the terms $\hat{h}_{zz}$, $\hat{h}_{xx} + \hat{h}_{yy}$, and $\hat{h}_{xy} - \hat{h}_{yx}$. The latter two can be turned into each other using a unitary transformation $e^{i\theta\tau^z}$ which commutes with $\mathcal{C}$ and $\mathcal{R}(\Phi)$. One may therfore without loss of generality restrict the analysis to $\hat{h}_{zz}$ and $\hat{h}_{xx} + \hat{h}_{yy}$ only, as we did in the main text. Depending on the relative magnitude of $\hat{h}_{zz}$ and $\hat{h}_{xx} + \hat{h}_{yy}$ one either finds a quadratic band touching ($\text{CFL}_{2\pi}$), or a gapped spectrum ($\text{CFL}_0$).

3. **Particle-hole and inversion symmetries.** When the rotation symmetry is broken down to twofold rotations (i.e., inversion), additional terms $\hat{h}_{xx} - \hat{h}_{yy}$ and $\hat{h}_{xy} + \hat{h}_{yx}$ are allowed. In the $\text{CFL}_{2\pi}$ regime, their effect is to split the quadratic band touching into two Dirac cones at different momenta. Inversion and particle-hole symmetries map these cones onto one another and protect them from opening a gap.

4. **Particle-hole symmetry only.** When particle-hole is the only symmetry present, $\hat{h}_{zx}$, $\hat{h}_{zy}$, $\hat{h}_{xz}$ and $\hat{h}_{yz}$ are also allowed and generically give rise to a gapped spectrum.

## DIAGONALIZATION OF $\mathcal{C}$- AND $\mathcal{R}(\pi/2)$-SYMMETRIC HAMILTONIAN

We consider the Hamiltonian $H_{\mathcal{R}} = \Psi_4^\dagger h_{\mathcal{R}} \Psi_4$ with

$$h_{\mathcal{R}}(\vec{k}) = \begin{pmatrix} -\Delta & ke^{-i\phi_k} & 0 & 0 \\ ke^{i\phi_k} & \Delta & 2g & 0 \\ 0 & 2g & \Delta & ke^{-i\phi_k} \\ 0 & 0 & ke^{i\phi_k} & -\Delta \end{pmatrix}, \quad (7)$$

where $ke^{i\phi_k} = k_1 + ik_2$. The eigenvalues of $h_{\mathcal{R}}(\vec{k})$ are

$$\begin{aligned} E_1(k) &= \sqrt{k^2 + g_+^2} + g, \\ E_2(k) &= \sqrt{k^2 + g_-^2} - g, \\ E_3(k) &= -\sqrt{k^2 + g_+^2} + g, \\ E_4(k) &= -\sqrt{k^2 + g_-^2} - g, \end{aligned}$$

where $g_\pm \equiv g \pm \Delta$ and $E_1 > E_2 > E_3 > E_4$ for $g > 0$. The corresponding normalized eigenvectors are given by

$$u_{1/3}(\vec{k}) = \frac{1}{\sqrt{2 + 2\frac{\left(g_+ \pm \sqrt{k^2+g_+^2}\right)^2}{k^2}}} \begin{pmatrix} e^{-i\phi_k} \\ \frac{g_+ \pm \sqrt{k^2+g_+^2}}{k} \\ \frac{g_+ \pm \sqrt{k^2+g_+^2}}{k} \\ e^{i\phi_k} \end{pmatrix}, \quad (8)$$

$$u_{2/4}(\vec{k}) = \frac{1}{\sqrt{2 + 2\frac{\left(g_- \mp \sqrt{k^2+g_-^2}\right)^2}{k^2}}} \begin{pmatrix} -e^{-i\phi_k} \\ \frac{g_- \mp \sqrt{k^2+g_-^2}}{k} \\ -\frac{g_- \mp \sqrt{k^2+g_-^2}}{k} \\ e^{i\phi_k} \end{pmatrix}. \quad (9)$$

## EVOLUTION OF BANDS FROM $\mathrm{CFL}_{2\pi}$ TO $\mathrm{CFL}_0$

Figure 1 shows the composite-fermion band structure for $g = \cos\alpha$, $\Delta = \sin\alpha$ over a range of $\alpha$. (i)-(iii) As $\alpha$ increases from zero, the curvatures of the positive and negative energy bands that meet at the quadratic band touching become unequal. (iv) The transition between $\mathrm{CFL}_{2\pi}$ and $\mathrm{CFL}_0$ occurs at $|\Delta| = |g|$ where three bands meet at one point. (v-viii) For $|\Delta| > |g|$ the spectrum is gapped, and the positive (negative) energy bands become degenerate at $g = 0$ .

## PSEUDOSPIN WINDING NUMBER

In the main text, we provided an argument why Berry phases of $\gamma_{\text{Berry}} = 0$ and $\gamma_{\text{Berry}} = 2\pi$ should be viewed as

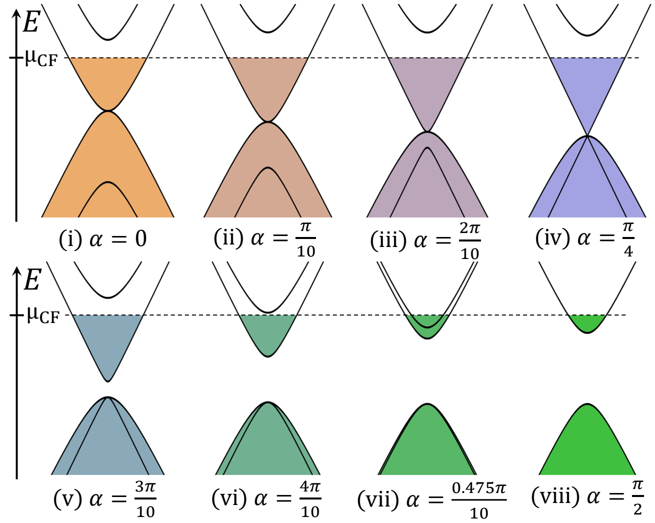


FIG. 1. Composite-fermion band structure shown for parameters $g = \cos\alpha$, $\Delta = \sin\alpha$.

distinct. Alternatively, one may sharply distinguish between $\mathrm{CFL}_{2\pi}$ and $\mathrm{CFL}_0$ band structures via a *pseudospin* $\hat{n}$ with

$$\hat{n} = \begin{pmatrix} \hat{h}_{xx} - \hat{h}_{yy} \\ \hat{h}_{xy} + \hat{h}_{yx} \end{pmatrix}, \quad (10)$$

where $\hat{h}_{\alpha\beta}$ are defined in Eq. (6). Evaluating $\hat{n}$ for the eigenstates $|u_j(\vec{k})\rangle$ of the $\mathcal{C}$- and $\mathcal{R}(\pi/2)$-invariant Hamiltonian, Eq. (7), we find

$$\langle u_j(\vec{k})|\hat{n}|u_j(\vec{k})\rangle = f_j\left(\vec{k}\right) \begin{pmatrix} \cos 2\phi_k \\ \sin 2\phi_k \end{pmatrix}. \quad (11)$$

In the $\mathrm{CFL}_{2\pi}$ regime, $g > |\Delta|$,

$$\lim_{\vec{k}\to 0} (f_1, f_2, f_3, f_4) = (0, -1, 1, 0), \quad (12)$$

while in the $\mathrm{CFL}_0$ regime, $\Delta > g > 0$,

$$\lim_{\vec{k}\to 0} (f_1, f_2, f_3, f_4) = (0, 0, 1, -1). \quad (13)$$

Consequently, the partially filled band, $j = 2$, features a winding of the pseudospin in $\mathrm{CFL}_{2\pi}$ that is absent in $\mathrm{CFL}_0$.

## PROJECTION ONTO QUADRATICALLY TOUCHING BANDS

To make the nature of $\mathrm{CFL}_{2\pi}$ more transparent, it is convenient to focus on the two bands that touch quadratically. Writing $\Psi_4^T = (\psi_1, \psi_2, \psi_3, \psi_4)$, the states created by $\psi_1$ and $\psi_4$ form a degenerate subspace at $\vec{k} = 0$. The corresponding states at small but non-zero $|\vec{k}| \ll |g| - |\Delta|$ are created by

$$\psi_+ = \psi_1 + \frac{ke^{i\phi_k}}{2g_+g_-}\left(\Delta\psi_2 - g\psi_4\right) \tag{14}$$

$$\psi_- = -\psi_4 + \frac{ke^{i\phi_k}}{2g_+g_-}\left(g\psi_2 - \Delta\psi_4\right). \tag{15}$$

Projecting the Hamiltonian of Eq. (7) onto the two-dimensional subspace spanned by $\psi_\pm$ yields

$$Ph_{\mathcal{R}}(\vec{k})P = \frac{1}{2g_+g_-}\begin{pmatrix} k^2\Delta & e^{-2i\phi_k}gk^2 \\ e^{2i\phi_k}gk^2 & k^2\Delta \end{pmatrix}. \tag{16}$$

The PH-breaking mass term $\sigma^z$ projects as

$$P\sigma^z P = \begin{pmatrix} 1 & 0 \\ 0 & -1 \end{pmatrix} + \mathcal{O}(k^2). \tag{17}$$

The fields $\psi_+, \psi_-$ transform under PH symmetry and rotations as

$$\mathcal{C}\psi_\pm\mathcal{C}^{-1} = -\psi_\mp, \tag{18}$$

$$\mathcal{R}(\Phi)\psi_\pm\mathcal{R}^{-1}(\Phi) = e^{\pm i\Phi}\psi_\pm, \tag{19}$$

which for $\Psi_2^T = (\psi_+, \psi_-)$ gives Eq. (16).

## BERRY CURVATURE INDUCED IN $\mathrm{CFL}_0$ BY PH SYMMETRY BREAKING

To estimate the Berry curvature induced in $\mathrm{CFL}_0$ by weak breaking of PH symmetry, we consider the limit $\Delta \gg g > 0$ and focus on the two positive energy bands with wave functions $u_{1,2}(\vec{k})$ specified in Eqs. (8) and (9). Weak breaking of particle-hole symmetry $\sim m\sigma^z\tau^0$ with $m \ll g, \Delta$ modifies the wave-functions as

$$\tilde{u}_{1/2}(\vec{k}) = u_{1/2}(\vec{k}) \pm \frac{m}{4g}u_{2/1}(\vec{k}). \tag{20}$$

Using these to compute the Berry-flux enclosed in a Fermi-surface of radius $K_F \ll \Delta$ one finds

$$\gamma_{\text{Berry}} = -2\pi\frac{m}{g}\frac{K_F^2}{8\Delta^2} \tag{21}$$

where we expanded to leading order in $K_F$ [cf. Eq. (17) from the main text].


[1] J. C. Y. Teo and C. L. Kane, Phys. Rev. B **89**, 085101 (2014).
[2] T. Senthil and M. Levin, Phys. Rev. Lett. **110**, 046801 (2013).
[3] Y.-M. Lu and A. Vishwanath, Phys. Rev. B **86**, 125119 (2012).
[4] S. D. Geraedts and O. I. Motrunich, Annals of Physics **334**, 288 (2013).